AIMS Environmental Science

AIMS Environmental Science, 12(1): 137–164.
DOI: 10.3934/environsci.2025007
Received: 27 July 2024
Revised: 14 October 2024
Accepted: 11 February 2025
Published: 20 February 2025

https://www.aimspress.com/journal/environmental

Research article

Development of new dielectric models for soil moisture content using mixture theory, empirical methods, and artificial neural network

Hashem Al-Mattarneh[1,*], Rabah Ismail[2], Adnan Rawashdeh[3], Hamsa Nimer[1], Mohanad Khodier[1], Randa Hatamleh[1], Dua'a Telfah[1], and Yaser Jaradat[1]

[1] Department of Civil Engineering, Yarmouk University, Irbid 21163, Jordan
[2] Department of Civil Engineering, Jadara University, Irbid 21110, Jordan
[3] Department of Information Technology, Yarmouk University, Irbid 21163, Jordan

* **Correspondence:** Email: hashem.mattarneh@yu.edu.jo; Tel:+962797417257.

Abstract: Environmental, geotechnical, agriculture, and water resources engineers all rely on accurate measurements of soil moisture content. The most widely used technique for determining soil moisture content is the electromagnetic method, which employs dielectric models to relate soil dielectric properties to its moisture levels. This paper introduces an innovative electromagnetic sensor designed to measure the dielectric properties of moist soil. The dielectric properties of seventeen coarse-grain soil samples and seventy-five samples with both coarse and fine grains at varying moisture contents, textures, and densities were measured. The findings were used to evaluate the effectiveness of the existing most common theoretical and empirical models for soil moisture measurement. The results show that all existing models have difficulties with accurately quantifying the soil moisture content. In response, this study developed three new types of dielectric models: a theoretical volumetric model, a general empirical model that addresses the shortcomings of existing models, and an artificial neural network (ANN) model, which demonstrated a higher potential for accurately predicting soil moisture content. The best new theoretical volumetric model was the power model, with a power of 0.9 for the dielectric constant and 1.4 for the loss factor. The best new general empirical model developed in this study considered soil density, texture, and moisture, achieving correlation coefficients of 97.6% for the dielectric constant and 97.2% for the loss factor. The developed ANN models to predict the dielectric properties of moist soil provided high correlation coefficients of more than 98.5%.

Keywords: soil; moisture content; electromagnetic sensor; dielectric model; artificial neural network

1. Introduction

The uppermost layer of the Earth's crust is made up of soil, which is a mixture of organic matter, minerals, water, air, and living things. The environment and human societies depend on the functions and services provided by the dynamic soil system. Soil is the premise for nourishment and biomass generation. Soil stores, and changes a huge assortment of substances, including water, inorganic, and natural compounds. Soil gives crude materials for human utilization [1]. It too serves as the premise for human exercises such as scene and heritage. It is also critical for our technical and socio-economic foundation, to deliver materials for their usage and support [2]. For the construction of buildings, the fields of agriculture, hydrology, meteorology, and civil and geotechnical engineering depend heavily on the moisture content of the soil [3]. Expanding the capabilities of well-established sensors and modeling methods to estimate soil moisture presents a challenge [4]. For a wide range of applications, such as better irrigation scheduling forecasting and breaking down rainfall into its runoff and infiltration components, data regarding soil moisture is required. One important factor that influences the engineering behavior of soils, particularly cohesive soils, is their moisture content. Soil moisture content also affects the pollution transport through soil material and the potential contamination of groundwater. As a result, one of the most important tasks in an experimental study in the fields of geotechnical and environmental engineering is to monitor and determine the moisture content [5].

There are several methods for measuring the water content of soil, both direct and indirect. A fundamental calibration technique used to compare various methods with one another is the standard method (gravimetric method) [6]. This technique is frequently used to calculate the moisture content of soil. A known-volume soil sample must be oven-dried for several hours at 105 degrees Celsius until reaches constant weight. The weight of the oven dry condition is subtracted from the initial field soil weight to determine the water content. The percentage of water by volume or weight can be used to express the moisture content. Even though it's a standard procedure and can provide a high level of accuracy, it takes a long time, costs a lot of money, destroys samples, and can't measure moisture over time or for large field investigations. Put simply, soil moisture measurements using the gravimetric method are impractical for hydrological and agricultural applications where frequent, large-scale in-situ observations are necessary. They are also less suitable for validating remote sensing products, which require data collected within a narrow time window aligned with satellite overpasses.

The indirect methods are invasive method called non-destructive testing (NDT). NDT approaches capable of directly gauging moisture levels, yielding precise outcomes with increased accuracy and resolution, are crucial for deepening our grasp of soil water dynamics and accurately determining its moisture content [7]. Several NDT methods have been developed to measure soil moisture content. The most available used NDT methods include:

- Neutron method: This method uses a relatively expensive radioactive source that requires a trained operator. It is also hazardous to the health and environment [8].
- Gamma-ray method: This is a non-destructive radioactive method. The application of this technique in the field is limited due to its high cost and complexity of use [9–10].
- Gypsum block method: This is a type of electrochemical cell. The primary constraint of this methodology is the gypsum block's dissolution and degradation, which necessitates periodic recalibration [11].
- Tensiometer method: Without upsetting the soil, it can provide continuous measurements of soil moisture. However, investigation has shown that tensiometers are not appropriate for use in dry soils. The use of this method in research is restricted by its high maintenance requirements [11].

- Time domain reflectometer (TDR): TDR is a non-destructive method that requires comparatively less labor; the instrument is safe to use, portable, and easy to install. The environment affects TDR probes. Therefore, gaps between the soil and the probe could cause inaccurate measurements. In extremely salinized soils, its applicability is restricted [12].
- Remote sensing methods: The electromagnetic energy that is reflected or emitted from the soil surface is necessary for the remote sensing of soil moisture. Although it is expensive and complex, remote sensing works best for larger areas that must be uniformly and repeatedly covered. Determining the water content of soil in dense vegetation is still a challenging task [13].
- Pressure plate method: Estimating the field capacity, permanent wilting point, and moisture content at various pressures is typically done using this method. At low water potentials, the apparatus is prone to errors. The approach overestimates [14].
- Ground penetrating radar (GPR): The transmission and reflection of electromagnetic waves through soil is the basis for GPR measurements. GPR is a high-resolution, quick, and non-destructive method that can cover a wide area and go beyond the surface layer. Because of the large sizes of the antennas, their use is restricted to steep and rocky slopes. GPR is challenging to use in forests because trees act as reflectors, producing inaccurate data [15–16]. Electromagnetic electrode method: This technique is heavily utilized for determining the moisture content of soil and for many other applications involving diverse fields and materials [17–21]. The electrode can be easily modified to fit the testing conditions using this straightforward method. Moreover, this electrode method is portable, low price, and capable of operating across a large frequency range. Numerous investigations were carried out to apply this philosophy to soil pollution, water quality, concrete moisture, and wood testing for strength and moisture [22–28]. The methods used to determine soil moisture content are summarized in Table 1, which also highlights the advantages and limitations of each method.

Soil moisture plays a key role in various hydrological applications, each requiring measurements across different spatial scales, from point measurements at monitoring stations to field, watershed, and regional scales. Accurate soil moisture readings at these scales are critical to meet the technical needs of tasks like state initialization, data assimilation, model parameter optimization, and model validation [29]. Yet, obtaining a representative average soil moisture value beyond the point scale is challenging. The distribution of soil moisture across different scales is influenced by factors such as soil texture, vegetation, terrain, and variations in precipitation [30]. Therefore, in-situ soil moisture measurements at multiple locations within the selected scale are essential for a reliable average estimate.

The most popular technique for determining the moisture content of soil and various other materials are the electromagnetic methods. The interaction between electromagnetic waves and soil material depends on the complex permittivity (ε*) and complex permeability (μ*) of soil. Since most soil is a nonmagnetic material, its permeability remains constant, allowing it to be characterized solely by its complex permittivity. The complex permittivity of soil (ε*) can be determined by subtracting the imaginary part of the soil's loss factor ($j\varepsilon''_{soil}$) form its dielectric constant (ε'_{soil}) [31]. The dielectric constant, signifying the extent of energy absorbed by the soil from the electromagnetic signal, and the loss factor indicates the energy loss from the electromagnetic signal due to current conductance. However, creating electromagnetic sensors to gauge soil moisture content remains challenging. These sensors use dielectric models of moist soil, but it is difficult to generalize these models to apply to all soil types. Important factors like soil density and texture, which affect the dielectric properties of soil,

are not adequately considered by the current dielectric models [17,32]. Consequently, significant errors may arise when predicting soil moisture content using the existing empirical models.

Table 1. Summary of methods used to determine soil moisture content.

Method	Advantages	Disadvantages and limitations	Ref.
Gravimetric method	The standard method, it is a reference to calibrate all other methods	It time time-consuming, costly, and mostly destroys the samples	[6]
Neutron method	Good accuracy	Relatively expensive, required trained operator, hazardous to the health	[8]
Gamma-ray method	Non-destructive radioactive	The Application in the field is limited by its high cost and complexity of use	[9,10]
Gypsum block method	Electrochemical with acceptable accuracy	Dissolution and degradation gypsum is the main constraint, and needs recalibration	[11]
Tensiometer method	Provide continuous measurements, and nondestructive	Not appropriate for low moisture and dry soils. Required high maintenance	[11]
Time domain reflectometer (TDR)	Nondestructive method, requires less labour; safe to use, easy to install	Air gaps between the soil and the probe cause error, it is not accurate for salinized and organic	[12]
Remote sensing method	Works best for larger areas that must be uniformly and repeatedly covered.	It is expensive and complex, remote sensing Determining the water content of soil in dense vegetation is a challenging task	[13]
Pressure plate	It is accurate for low water content	The method is prone to errors and the approach overestimates water content	[14]
Ground penetrating radar (GPR)	GPR is a high-resolution, quick, and non-destructive method that can cover a wide area and go beyond the surface layer.	GPR is challenging to use in forests because trees act as reflectors, producing inaccurate data	[15,16]
Electromagnetic electrode method	The electrode can be easily modified to fit the testing conditions. It is portable, low-priced, and operates at a wide frequency range	Needs to model the circuits for the design of electrodes, it is costly at high frequency.	[17–21]

Calibration is a vital process that adjusts sensor readings to account for soil-specific conditions, ensuring accurate and consistent soil moisture measurements. For instance, soils with higher clay content generally show higher electrical conductivity, whereas sandy soils typically exhibit lower conductivity. This variation can significantly impact the accuracy of soil moisture sensors. Therefore, developing a reliable calibration for dielectric-based sensors must carefully consider both the sensor's

operating frequency and the soil type where measurements will be taken [12,33].

For applications needing frequent soil moisture readings, modern tools like electronic sensors that give instant measurements are essential. These sensors generally measure the dielectric properties of soil and water, using this information to estimate moisture levels through specific calibration relationships. Although many calibration methods for these sensors are available in scientific literature, their field use is often limited due to calibration difficulties, technical complexity, and doubts about their accuracy. This study aims to develop a multi-array electromagnetic sensor (MAES) to precisely measure the soil dielectric properties. The primary goal is to measure the dielectric properties of soils with different grain sizes, textures, and densities at various moisture contents. Additionally, the study aims to evaluate the most commonly used dielectric models for soil moisture content. Furthermore, new theoretical and empirical dielectric models will be developed for improved accuracy. Finally, the study will explore the use of artificial intelligence (AI), employing different ANN models, to predict soil moisture content more accurately.

2. Dielectric models for soil material

Several theoretical and empirical physical dielectric models have been developed using three approaches namely; the Phenomenological approach, mixture volumetric approach and empirical statistical approach [34–37]. The following subsection explain briefly these three approaches. Furthermore, AI using ANN modeling will be added to model soil dielectric properties.

2.1. Phenomenological models

It is evident from the review of phenomenological models such as Cole-Cole [38] and Debye [39] that require recalibration for every unique material. As such, it is challenging to describe the dielectric differences between different types of soil using these models. Therefore, these types of models are not used for soil moisture practical applications [7].

2.2. Mixture volumetric models

Based on the relative concentrations of the various soil constituents and each one's distinct dielectric properties, volumetric models characterize the dielectric properties of a soil. Pore space, volumetric water content, and solid matter are the three primary input parameters used in these models [7]. For soil moisture content, multiple three-phase mixture volumetric models were created. These stages included solid particles, water, and air. These phases' volume fractions are, respectively, θ_a, θ_w, and θ_s for air, water, and solid. For air, water, and solid phases, the corresponding dielectric properties are ε_a, ε_w, and ε_s. The following are the most widely used theoretical mixture models for determining soil moisture content:

Silberstein's linear model was suggested [40]. Eqs (1) and (2) provide the dielectric constant and loss factor formulas, respectively.

$$dielectric\ constant = \varepsilon'_{soil} = \theta_s \varepsilon'_s + \theta_w \varepsilon'_w + \theta_a \varepsilon'_a \quad (1)$$

$$loss\ factor = \epsilon''_{soil} = \theta_s \epsilon''_s + \theta_w \epsilon''_w + \theta_a \epsilon''_a \quad (2)$$

Birchak's square root model (power equal to 0.5) [41]. Eqs (3) and (4) provide the dielectric constant and loss factor formulas, respectively.

$$dielectric\ constant = (\varepsilon'_{soil})^{1/2} = \theta_s (\varepsilon'_s)^{1/2} + \theta_w (\varepsilon'_w)^{1/2} + \theta_a (\varepsilon'_a)^{1/2} \quad (3)$$

$$loss\ factor = (\varepsilon''_{soil})^{1/2} = \theta_s (\varepsilon''_s)^{1/2} + \theta_w (\varepsilon''_w)^{1/2} + \theta_a (\varepsilon''_a)^{1/2} \quad (4)$$

Looyenga's power model states that power equals 1/3 [42]. Eqs (5) and (6) provide the dielectric constant and loss factor formulas, respectively.

$$dielectric\ constant = (\varepsilon'_{soil})^{1/3} = \theta_s (\varepsilon'_s)^{1/3} + \theta_w (\varepsilon'_w)^{1/3} + \theta_a (\varepsilon'_a)^{1/3} \quad (5)$$

$$loss\ factor = (\varepsilon''_{soil})^{1/3} = \theta_s (\varepsilon''_s)^{1/3} + \theta_w (\varepsilon''_w)^{1/3} + \theta_a (\varepsilon''_a)^{1/3} \quad (6)$$

The logarithmic model that Lichtenecher proposed [43]. Eqs (7) and (8) provide the dielectric constant and loss factor formulas, respectively.

$$DC = \varepsilon'_{soil} = \theta_s \ln \varepsilon'_s + \theta_w \ln \varepsilon'_w + \theta_a \ln \varepsilon'_a \quad (7)$$

$$DL = \varepsilon''_{soil} = \theta_s \ln \varepsilon''_s + \theta_w \ln \varepsilon''_w + \theta_a \ln \varepsilon''_a \quad (8)$$

Among these mixture models, a general power model was used for several materials with different powers. The researcher sought to determine the power to best fit the experimental data. The power mode for dielectric constant and dielectric loss are given in (9) and (10).

$$(DC)^{\alpha} = (\varepsilon'_{soil})^{\alpha} = \theta_s (\varepsilon'_s)^{\alpha} + \theta_w (\varepsilon'_w)^{\alpha} + \theta_a (\varepsilon'_a)^{\alpha} \quad (9)$$

$$(DL)^{\alpha} = (\varepsilon''_{soil})^{\alpha} = \theta_s (\varepsilon''_s)^{\alpha} + \theta_w (\varepsilon''_w)^{\alpha} + \theta_a (\varepsilon''_a)^{\alpha} \quad (10)$$

The volume fraction of the soil phases and the dielectric characteristics of each phase were necessary for all of these mixture models. Furthermore, these models fail to take into account the interactions between these soil phases, which renders them inaccurate for estimating soil moisture content. The solid soil particles and the water phases may interact chemically or physically. These interactions are not taken into consideration in any of these models.

2.3. Statistical and empirical models

The empirical model is a statistical and mathematical representations of the correlations between a medium's other attributes its texture and volumetric water content—and its dielectric properties. The mathematical description does not seem to have a physical foundation. An empirical model might therefore only hold true for the data that were utilized to establish the relationship. The study of soil moisture content has served as the basis for numerous empirical models.

Many models that researchers have proposed rely on their experimental work, data fitting, and model parameter determination. There is no standard formula for empirical models; instead, the best

statistical regression model to fit the data must be found through multiple trials. To select the best model from the trials, one must perform an ANOVA analysis and ascertain the correlation coefficient, error, F-test, and level of significance.

The most widely accepted empirical dielectric model for soil moisture content was proposed by Topp [44]. When the soil has a varied texture, and contains organic matter, salt, and other characteristics, the Topp model is unable to measure the soil accurately. The formula for the Topp model is (11).

$$Water\ content = \theta_w = -5.3 \times 10^{-2} + 2.29 \times 10^{-2}\varepsilon_{soil} - 5.5 \times 10^{-2}\varepsilon_{soil}^2 + 4.3 \times 10^{-6}\varepsilon_{soil}^3 \quad (11)$$

2.4. AI Using ANN models

The relationship between dielectric properties and soil composition and properties is determined using theoretical dielectric models including mixture theory, phonological models, and empirical models using central composite and response surface methodology. There are several problems associated with these models and methods such as complications of soil material, unavailability of needed soil information, complicated nonlinear relationship, and limited application of statistical methods to the condition of soil used to develop these models. ANN shows promising capabilities of overcoming such problems in many fields [45].

ANN models have been used for several applications for the prediction of the composition of various materials including soil. ANN has been found to offer good modeling techniques in many areas of soil material including, prediction of soil consolidation [46], prediction of soil organic matter [47] estimation of the shear strength of soil [48] prediction of soil compaction [49–50], estimation of soil moisture [51], prediction of soil permeability [52], and soil pollution such as heavy metal and hydrocarbon [53–54]. Moreover, ANNs have been used in other vital applications including the prediction of carbon emissions [55] and their real-time development [56].

Among the information-driven modeling tools that may capture complicated and nonlinear interactions between input and output datasets without requiring a prior understanding of the underlying phenomena are artificial neural networks (ANNs). ANNs have a flexible statistical structure. Three or more layers are usually present in these networks: an input layer, hidden layers, and an output layer. The neurons of the primary hidden layer receive all input data from the input layer [57].

When producing outputs that match predetermined inputs, the output layer is essential. In the meantime, sets of feature detectors are performed by the hidden layers, which might consist of one or more layers. In system modelling, choosing the right network framework is an important but difficult challenge [58–60]. A schematic illustration of a general 3-layer ANNs model is shown in Figure 1.

Applying ANNs can be done in a variety of ways and deducing which one works best is hard because it involves systematically testing a lot of different scenarios. There are several different types and frameworks of ANNs, such as Regression Neural Networks, Multilayer Perceptron Networks, Probabilistic Neural Networks, Radial Functions Networks (RFN), Back Propagation Networks (BPN), Cascade Neural Networks (CNN) and Feedforward Neural Networks (FNNs). The most widely used of these are FNNs and CNN [61,62]. Therefore, these two ANN models will be used in this study.

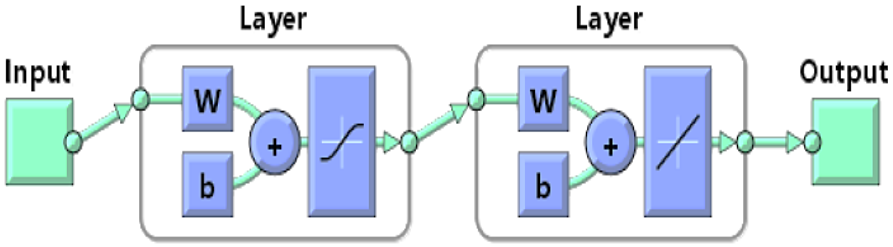

Figure 1. A schematic representation of a general 3-layer ANNs model.

The creation of an Artificial Neural Network model to investigate the connections between the soil complex permittivity and the four soil phases including solid, water and air, is one of the study's two primary goals. To control soil moisture content and predict the total water level, it is essential to comprehend the relationship between soil dielectric constant, dielectric loss, and volume fraction of soil phases. The second goal is to employ the ANN to forecast the soil moisture content by using the soil's measured dielectric constant and dielectric loss.

3. Multi-array electromagnetic sensor

The new MADS for estimating soil moisture is presented in this section. The capacitive parallel plate dielectric cell (CPPDC) created in earlier research [19,31], was used to calibrate the new sensor because it has the ability to precisely compute the dielectric characteristics of a variety of materials, including composite material, liquids, and geotechnical materials like as rock and soil. The following subsection presents the MADS's detailed design.

3.1. Preliminary design of MADS

A number of designs were established, and their appropriateness for the in-situ was assessed. The dielectric properties were not really assessed; instead, the only focus was on deciding their suitability for use in soil. Four configurations for the design and setup were explored: cone penetration rod, cylinder probe, plate probe, and pin probe.

The pin probe, shown in Figure 2a, was simply placed into the field; however, because the soil's electric field would not be consistent with the AC signal, there would be little contact of the probe and the sand, and the pine design was discarded. The second probe was the parallel plate design presented in Figure 2b enhanced the AC interaction with the soil by creating a steady uniform field, but it was not used because of large fringing of electrical field at the edges.

The cone penetration design, shown in Figure 3, was the final design that formed as coaxial rod and a ring. This particular design was selected due to its capacity to offer a satisfactory degree of soil interaction and its simplicity of insertion into the field. Furthermore, cone penetration tests like this design configuration were commonplace to geotechnical engineers. The probe provided the profile of dielectric measurements at various soil depths by enabling the use of multi-ring electrodes.

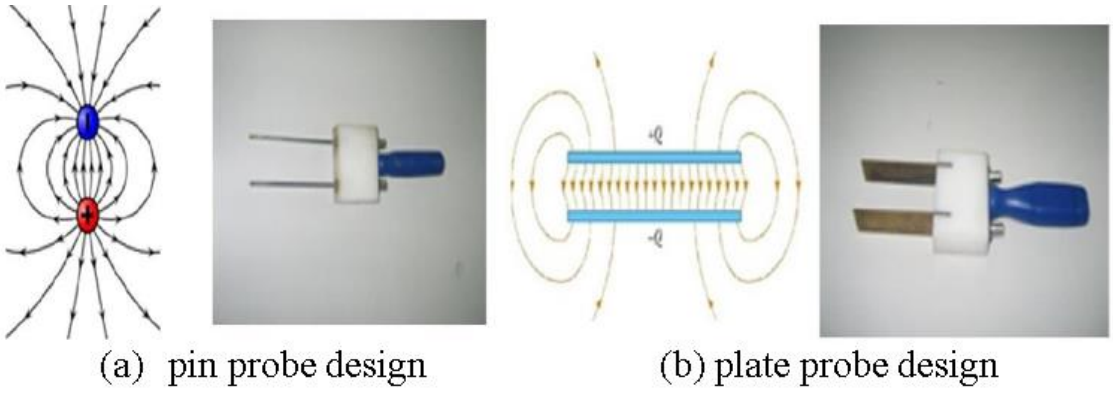

Figure 2. Schematic diagram and actual preliminary MAES (setup and design).

3.2. Final design of MAES

Because it is simple to insert for in situ testing, the cone penetration probe was selected as the final MADS design and configuration for soil moisture content implementations. Multi ring electrodes were used in the MADS setup and design, which allowed the electric field to extend both inside and outside the rod.

The impedance (Z) inside the sensor was constant, but the Z outside varied according to the attributes of the surrounding soil of rod and ring electrodes. The admittance (Y) of soil calculated from the equivalent model circuit of the MAES as inner impedance and outer impedance. The sensor's schematic diagram is shown in Figure 3a.

An LCR meter was used in the final configuration and design of MAES to measure soil impedance and act as the source of the electromagnetic signal. The LCR meter was connected to the ring electrodes via coaxial cables, and for automated calculations, it was also connected to a personal computer. The actual MAES is given in Figure 3b.

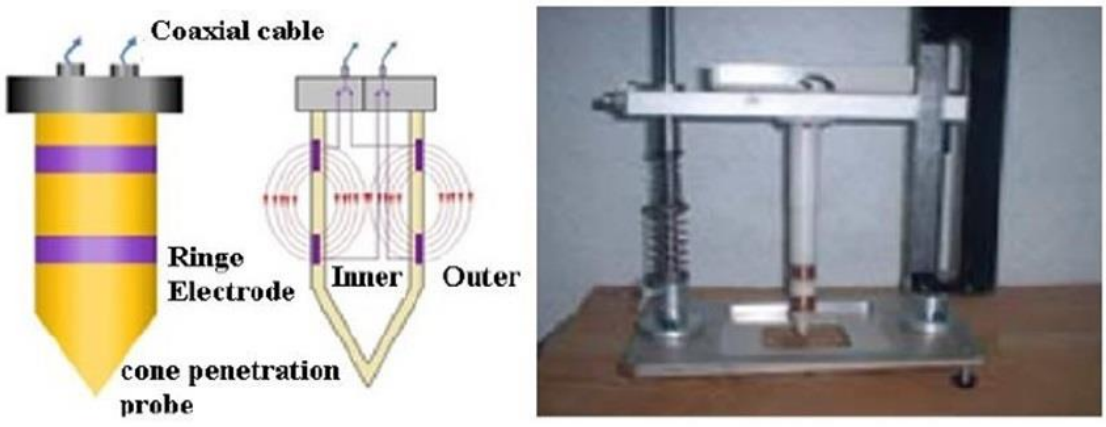

Figure 3. Schematic diagram and actual cone probe design and setup.

3.3. Final design of MAES

The complex *Y* of soil is determined by measuring the impedance of the soil surrounding the dielectric sensor at each frequency using an LCR meter. Using (12), one could determine the Y of the soil neighboring the sensor based on the soil *Z*.

$$Y_{soil} = \frac{1}{Z} = Y'_{soil} + iY''_{soil} = G_{soil} + iB_{soil} \tag{12}$$

The measured real part (*G*) and imaginary part (*B*) of soil Y could be used to calculate the real and imaginary parts of the complex permittivity of soil, also known as the ε' and ε'' determined, respectively, using (13) and (14).

$$Dielectric\ constant = \varepsilon'_{soil} = \left(\frac{B_{soil}}{\omega C_o} - \frac{C_{in}}{C_o}\right) \tag{13}$$

$$Loss\ factor = \varepsilon''_{soil} = \left(\frac{G_{soil}}{\omega C_o}\right) \tag{14}$$

Where C_{in} is the inside capacitance, C_o the capacitance of free space, and ω is the angular frequency and given by (15).

$$\omega = 2\pi f \tag{15}$$

Where f is the frequency in hertz. To compute the dielectric properties as mentioned in (13) and (14), the sensor constant C_o and C_{in} for any operating frequency must be ascertained. Two materials with known ε' and ε'' were used to find these two sensor constants. The sensor parameters could be found by solving the two linear equations that result from these two measurements, which are represented by (16) and (17).

$$B_{material\ one} = \omega\ (\varepsilon'_{material\ one}\ C_{\ o} + C_{\ in}) \tag{16}$$

$$B_{\ material\ two} = \omega\ (\varepsilon'_{material\ two}\ C_{\ o} + C_{\ in}) \tag{17}$$

The dielectric sensor parameters were determined at each frequency using methyl alcohol and deionized water. Methyl alcohol and deionized water had complex permittivity of 9.02-i7.10 and 80.2-i0, respectively. To compute the dielectric properties of soil, the sensor constants C_o and C_{in} were calculated at every frequency between 1 kHz and 1000 kHz. These values were then stored.

3.4. Calibration and validation of MAES

The MADS was calibrated using two techniques. The LCR meter's open/short calibration standard method, created by HP, was the first technique used to calibrate the MADS [63]. After the open/short calibration standard was put into place, the measure impedance of Teflon, the standard material, was more accurate and the error between the measure and actual values dropped from 4.0 percent to less than 1.0 percent.

The CPPDC was the second calibration technique employed. Diesel served as the standard material, and its dielectric characteristics were assessed using the suggested MADS in addition to the

CPPDC. In order to calibrate MADS, the results of the diesel's dielectric properties using both CPPDC and MADS were compared. The results show that the value measured by CPPDC was greater than the measured dielectric properties using the suggested MADS. This was observed in a number of materials, with very tiny and nearly constant errors. To ensure that the material's measured dielectric properties match (have an equal value) with the measured values obtained using CPPDC, a correction factor was added. The correction factor is presented in (18)

$$Correction\ factor = \frac{\varepsilon'_{CPPDC}}{\varepsilon'_{using\ MAES}} \tag{18}$$

Validation of MAES: To confirm that MAES is accurate in measuring a material's dielectric characteristics. The dielectric characteristics of the water were computed after the sensor was submerged in it at 25°C. The outcomes show strong agreement with findings published by numerous researchers. If we take into account the possibility that the water may not be pure, the deviation between the computed dielectric constant of water and its reported value of 80.0 was below 1.0%.

4. Materials and methods

Sample preparation involved the use of two different types of soil: clay and sand. To get closer to the natural environment, which lacks pure sandy or clayey soil, various percentages of clayey and sandy soil were combined. Figure 4 lists the characteristics and grading of both clay and sandy soils. Two set of soil samples were used. The first set sandy soil was used and the moisture ranges from 0% to saturated condition 40%. This set of testing include 17 sand soil with different moisture content. The second set of soil samples were 75 soil samples. The soil samples contain sand and clay at different percentages. The moisture of the second soil set evaluated at 5 water level and five level of various texture and 3 level of soil density produced using three level of compaction. The detail of these soil sets are explained in the following subsections.

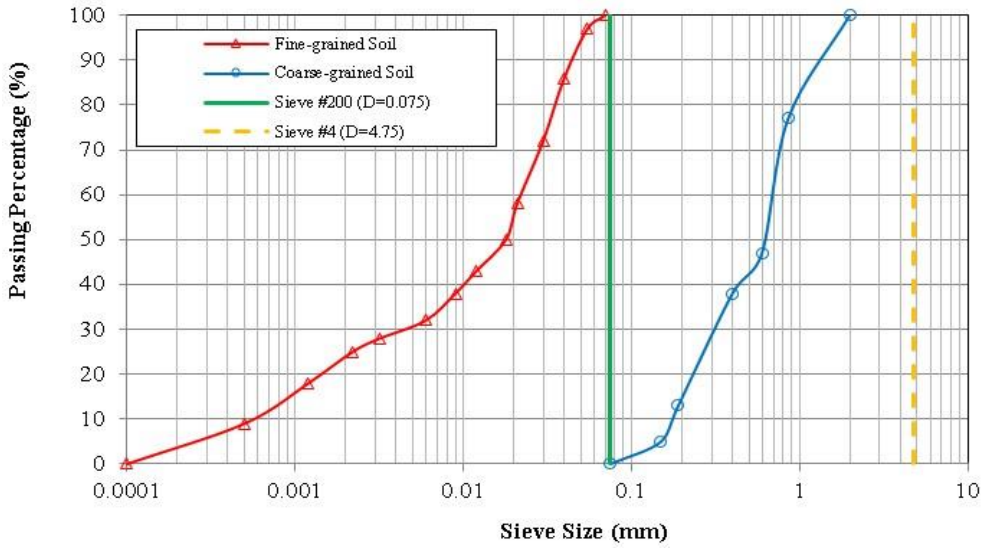

Figure 4. Grading characteristics of sand and clay soil samples.

4.1. Sandy soil samples and moisture content

The dielectric of sand (coarse-grained) was measured at different moisture contents, from 0.0 percent (oven dry condition) to 40.0 percent moist soil (saturated condition). A total of seventeen samples of sand (specific gravity=2.650) and varying moisture contents were prepared. Every model—theoretical, empirical, and AI—was assessed. It was possible to create new dielectric models for moist sandy soil.

4.2. Soil texture, soil density and water content

Five series of samples were prepared in order to assess the impact of soil moisture content, texture, and density. These series combine the fine-grained (clay) and coarse-grained (sand) contents to create a soil sample. There were five coarse-grained content by weight. 100 percent (pure coarse-grained), 75, 50, 25, and 0 percent of the contents were sand (coarse-grained). These five series' corresponding clay (fine-grained contents) were 100 (pure fine-grained), 25, 50, 75, and 0 percent. Because soil physical properties like water content, density, and porosity are dependent variables and affect each other, the dielectric properties of each series were measured and evaluated at five water content by volume. The water contents range from 0.0 to 20.0 percent with five percent increments. To better understand the effects of density and porosity, each soil sample was filled into the dielectric cell using three different levels of compaction, resulting in three different densities and three different porosities. The dielectric properties were measured at frequencies ranging from 1 to 1000 kH.

5. Results and discussions

The focus in this study was to develop three new dielectric model for moisture content of soil. First model will use the theoretical mixture volumetric approach and the second new model will use the empirical approach to include the effect of soil density and soil texture such as sand and clay content on the dielectric models of moist soil. The third model was the ANN model to determine the dielectric properties of moist soil.

5.1. Dielectric models for sandy soil

We prepared and tested seventeen samples of sandy soil (coarse-grained soil with specific gravit =2.65), varying in moisture content from 0.0 percent (oven-dry) to 40.0 percent (saturated condition). New dielectric models for moist sandy soil were developed after an evaluation of all theoretical, empirical, and AI models.

5.1.1. Volumetric dielectric mixture models

Three phases of mixture volumetric dielectric models of soil material were assessed. The three phases of soil are air, water, and solid. The dielectric characteristics of the soil constituents (phases) and the volume percentages of each constituent determine the dielectric property of the soil mixture volumetric dielectric. For soil materials, a number of theoretically feasible mixture dielectric models were created and put forth. The most advanced theoretical mixture volumetric models for soil

composition were examined. Silberstein, Birchak, Looyenga, and Lichtenecker are some of these models. These models were used to determine the dielectric constant and loss factor of soil based on the volume fraction of the constituent parts of the soil material and the dielectric characteristics of each phase (component). The computed dielectric constant and the extent to which these values match the experimental data at each moisture content were shown in Figure 5.

Using the previously mentioned analytical models, Figure 6 presents the result of the optimal theoretical model for the dielectric constant of clean soil at various moisture contents and compares it with the measured values from this study.

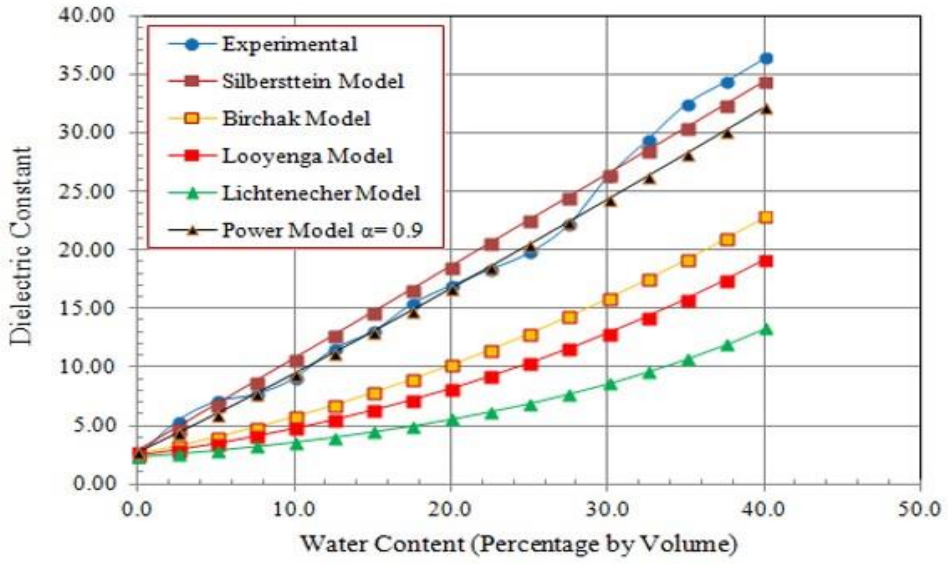

Figure 5. Experimental and available dielectric constant mixture models of sandy soil versus water content.

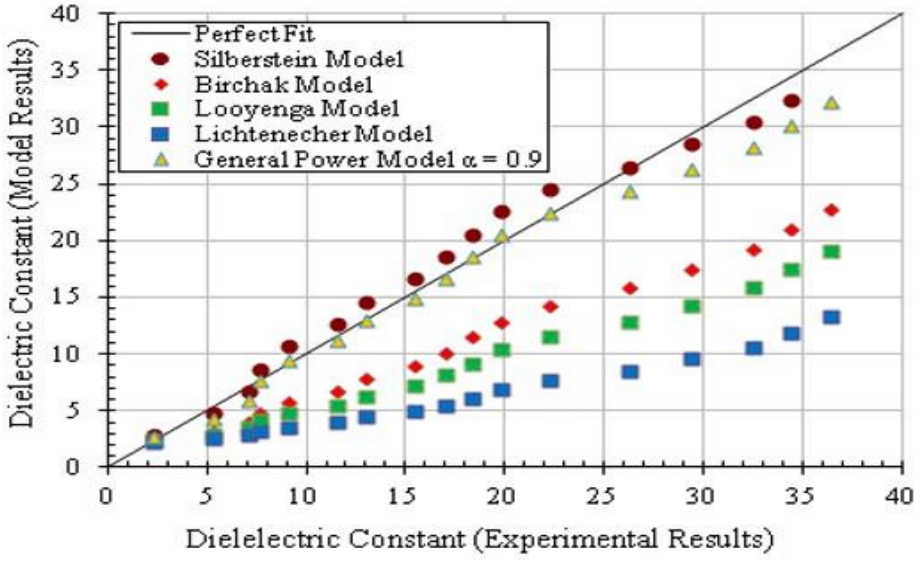

Figure 6. Experimental dielectric constant versus model dielectric constant.

Based on the proposed theoretical models, Figure 7 displays the loss factor of the sand samples. As seen in Figure 8, the best theoretical model was found by comparing the models that were given with the experimental values that were measured.

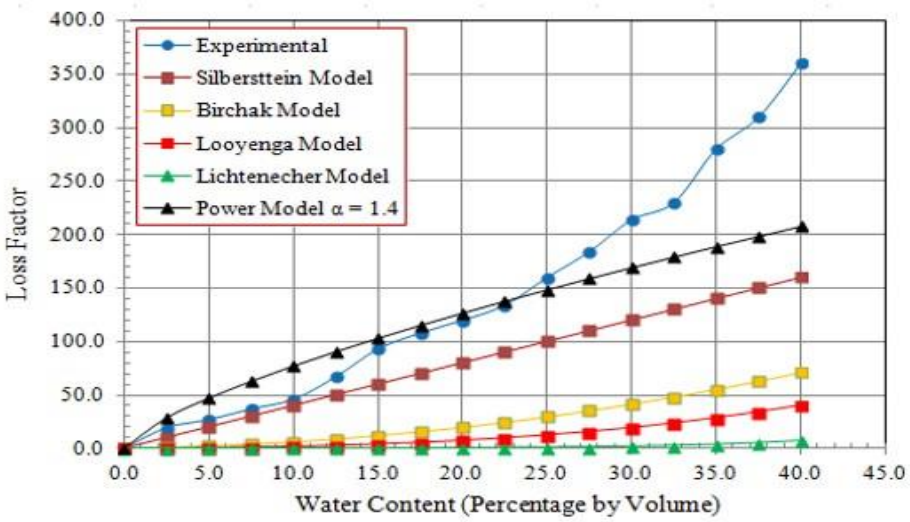

Figure 7. Experimental and available loss factor mixture models of sandy soil versus water content.

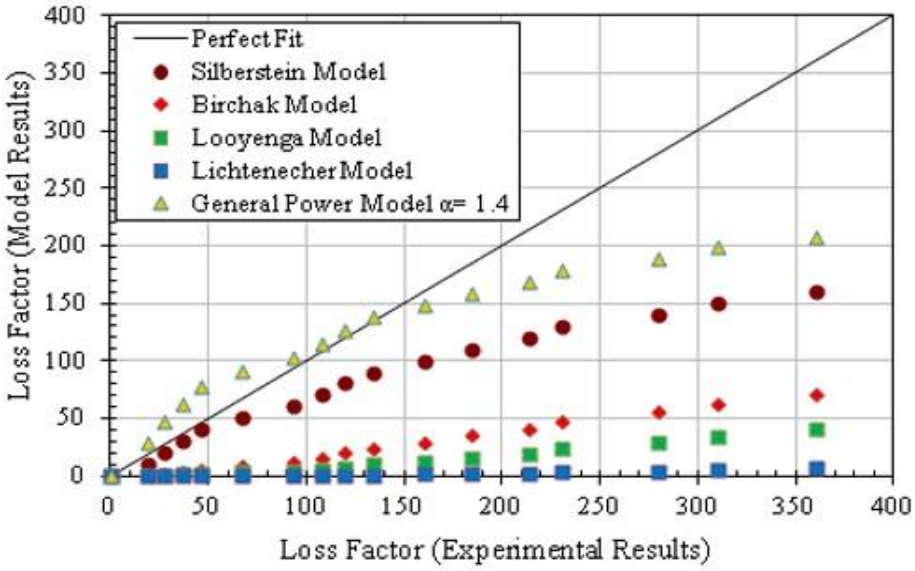

Figure 8. Experimental loss factor versus model dielectric constant.

According to the dielectric constant result using analytical soil models, Silberstein (linear) was the model that most closely fit the experimental data. The loss factor of moist soil was underestimated by all analytical models. New mixture volumetric dielectric models for the dielectric constant and loss factor were proposed in this study. The three-phase power model was one of the newly suggested models. At $\alpha = 0.9$ for the dielectric constant and 1.4 for the loss factor, the experimental measurement

fit the power function the best. The newly suggested model fit power model is given by (19) and (20) dielectric constant and loss factor respectively.

$$Dielectric\ constant = (\epsilon'_{soil})^{0.9} = \theta_s\,(\epsilon'_s)^{0.9} + \theta_w\,(\epsilon'_w)^{0.9} + \theta_a\,(\epsilon'_a)^{0.9} \quad (19)$$

$$Loss\ factor = (\epsilon''_{soil})^{1.4} = \theta_s\,(\epsilon''_s)^{1.4} + \theta_w\,(\epsilon''_w)^{1.4} + \theta_a\,(\epsilon''_a)^{1.4} \quad (20)$$

5.1.2. Empirical dielectric models

Several empirical models have been examined in order to develop the most appropriate model for determining the dielectric properties of soil materials, as analytical models are not able to provide accurate estimations of these properties. Numerous statistical models, including linear, quadratic, and cubic models, have been proposed by researchers to determine the relationship between the water content and the dielectric constant of soil. Regression analysis, both multilinear and multinonlinear, was performed on these models in this study using MATLAB.

Table 2 summarizes the regression analysis and model fitting, and Figure 9 shows the models with 95% confidence fitting curves. As can be seen in Table 2, where θ_w stands for the volume fraction of moisture content, the cubic model was found to be the best. This model had the lowest mean square error and the highest correlation coefficient (R^2 = 0.9937 and RMSE = 0.8478), similar to the one put forth by Topp [44]. Furthermore, of all the models examined, this one had the smallest and lowest residual value.

Table 2. Regression analysis and fitting performance of dielectric constant models.

Model	Correlation coefficient (R^2)	Adjusted correlation coefficient	Residual mean square error (RMSE)	F-value	P-Value Sig.
Linear model	0.9817	0.9817	1.4910	804.74	0.000
Quadraric model	0.9945	0.9937	0.8489	1257.38	0.000
Cubic model	0.9937	0.9937	0.8478	840.85	0.000

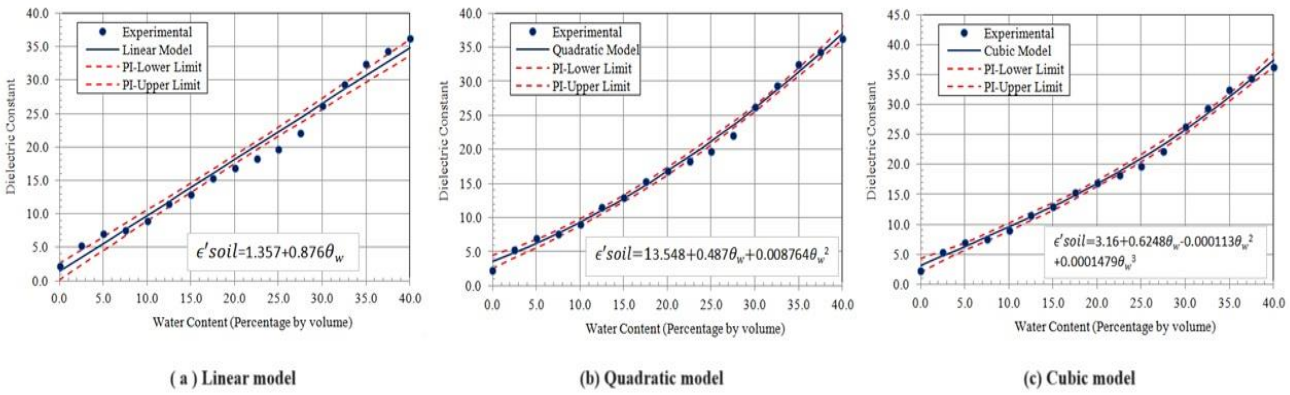

(a) Linear model (b) Quadratic model (c) Cubic model

Figure 9. Empirical dielectric constant models versus moisture content of sand soil.

On the other hand, a number of dielectric models for loss factor have been put forth by scientists to ascertain the connection between soil water content and loss factor. There are cubic, quadratic, and linear versions of these models. These models were created for this study, and Table 3 shows the results of the regression analysis and model fitting. Figure 10 displays the models with 95% confidence fitting curves. According to Table 3, the cubic model turned out to be the most effective. This model, which is comparable to Topp's model, had the lowest mean square error and the highest correlation coefficient (R^2 = 0.9975). This model also had the smallest and lowest residual value out of all the models that were looked at.

Table 3. Regression analysis and fitting performance of loss factor models.

Model	Correlation coefficient (R^2)	Adjusted correlation coefficient	Residual mean square error (RMSE)	F-value	P-Value Sig.
Linear model	0.9588	0.9561	22.72	804.74	0.000
Quadraric model	0.9949	0.9941	8.294	1257.38	0.000
Cubic model	0.9975	0.9969	6.059	840.85	0.000

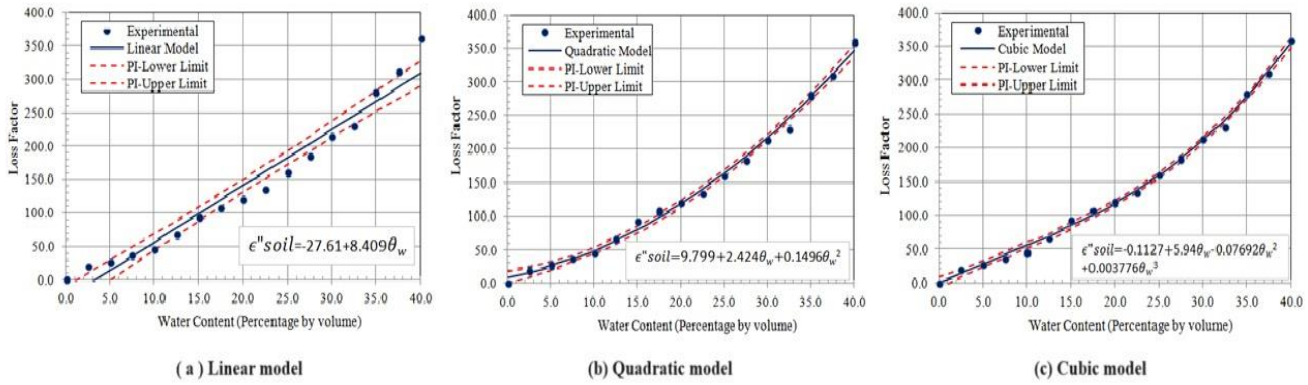

Figure 10. Empirical loss factor models versus moisture content of sand soil.

5.1.3. ANN dielectric models

To identify the most suitable artificial neural network (ANN) model for predicting soil moisture content and dielectric properties, several performance metrics were considered. These included the number of learning trials, correlation coefficients, mean square error, and residual error. Various activation functions were applied in the proposed feedforward neural network (FNN) models, including linear, hyperbolic tangent (tanh), logistic (or sigmoid), and Gaussian functions (see Figure 11). The primary role of an activation function is to introduce non-linearity to the neuron's output by calculating a weighted sum and applying bias, which determines whether the neuron is activated.

The soil sample data was divided into three groups for training, validation, and testing. The first group, representing 70% of the samples, was used to train the FNN and CNN models. The second group, consisting of 15% of the total samples, was used as a validation set to assess the performance of these models. The final 15% was reserved for testing and evaluating how well the ANN models fit

the data. This systematic division facilitated a robust evaluation and optimization of the ANN models for predicting dielectric properties using soil moisture content and soil phases.

Two ANN models were used to predict sand dielectric properties based on the measured sand moisture content using the proposed sensor. These models are FNN and CNN. FNN and CNN have been used in several engineering applications [64–66]. The schematic diagram and detail of ANN models is presented in Figure 11. The two models used an input layer with one variable (sand moisture content) and one output layer with two variables (sand dielectric constant and loss factor). The FNN model has one hidden layer with six neurons while the CNN model has one hidden layer with six neurons. Both models have used the 'logsig' activation function in the input and hidden layers. Both models also used the 'puelin' activation function in the output layers. The training method in both models was the 'levenberg Marquardt' method. The performance details of the used FNN models are shown in Figure 12. The best ANN model consist of three layers, input layer contains 1 neuron, one hidden layer contains 6 neurons, and output layer contains 2 neurons.

The prediction results of the dielectric properties of moist sandy soil using the ANN model indicated that both models are excellent in estimating dielectric properties. The correlation coefficients (R) of the training phase for FNN and CNN models were 0.9999 and 0.9816, respectively. Therefore, the best ANN was FNN. The R for the validation and testing phase of FNN were 0.9915 and 0.9830, respectively.

To further assess the reliability of the ANN models, multiple rounds of random training were conducted. This ensured that the promising results of the ANN models were not due to chance (i.e., a specific training case). Notably, the performance metric of correlation coefficients (R) showed no significant differences between the various training trials, confirming the consistency of the model's performance.

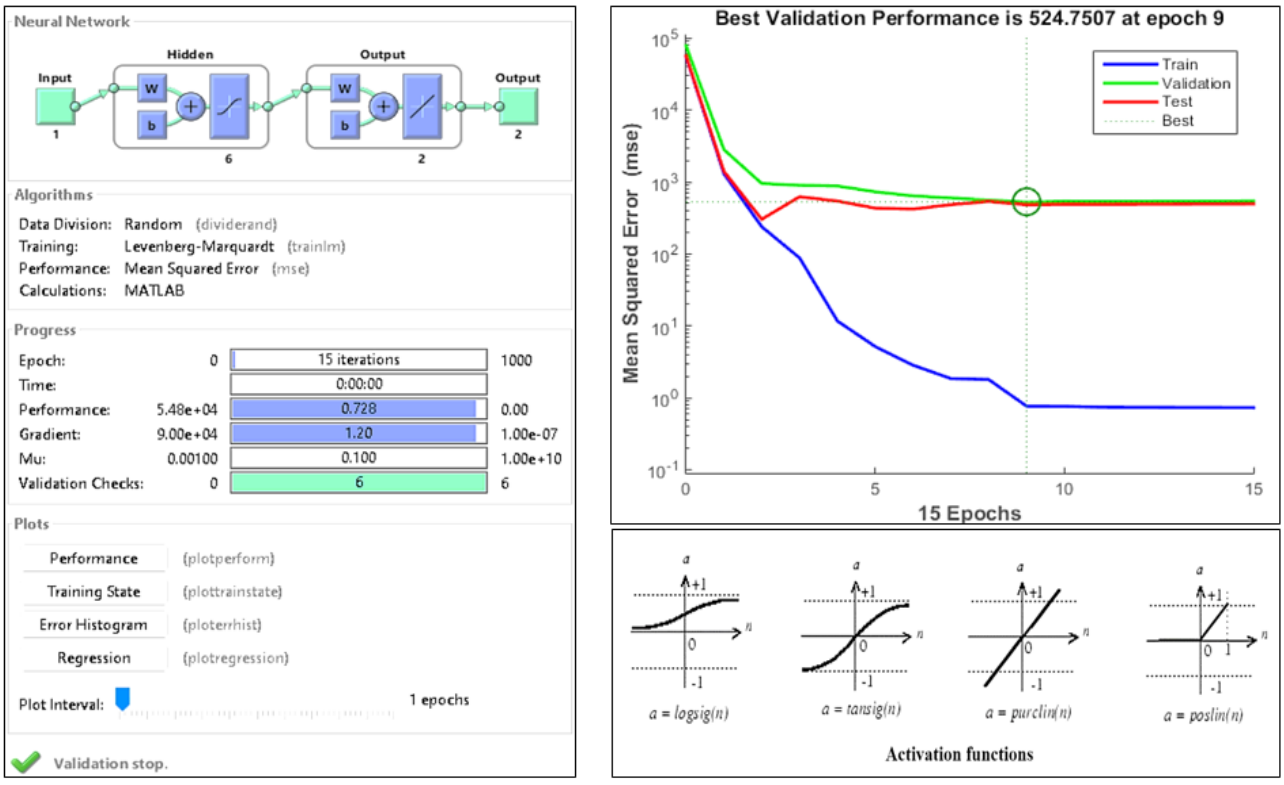

Figure 11. The detail of FNN model used to predict soil dielectric properties using moisture content.

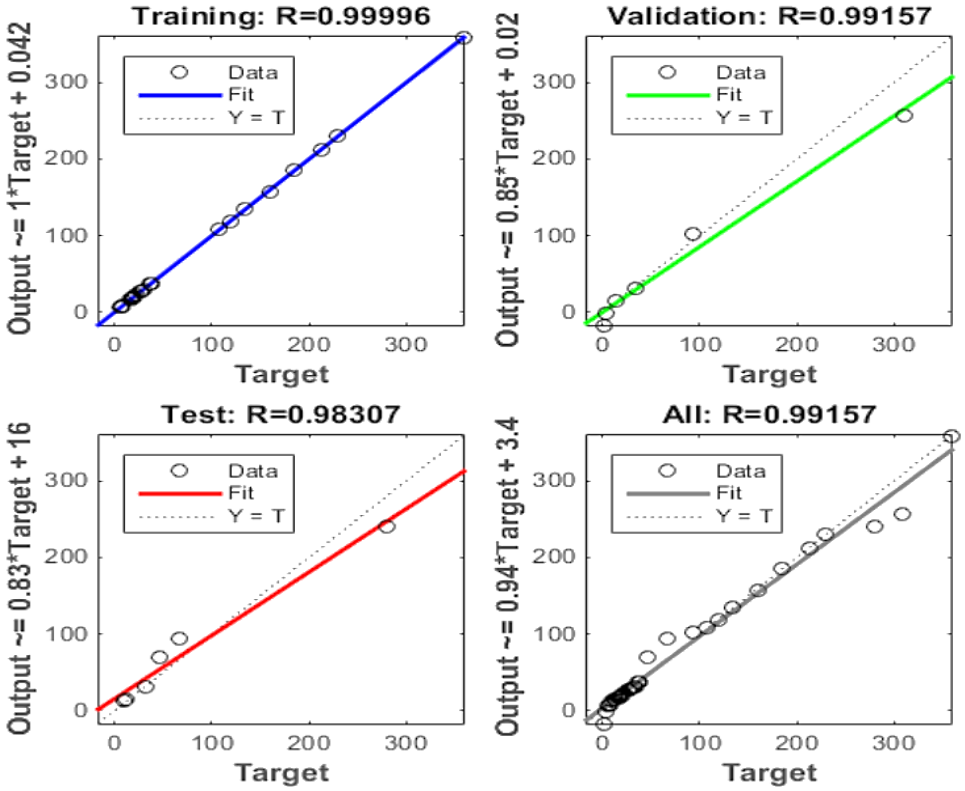

Figure 12. Experimental dielectric properties versus predicted values using FNN model.

5.2. Soil texture, soil density and moisture content

Seventy-five soil samples were prepared in order to test the effects of soil moisture content, soil texture, and soil density on soil dielectric properties. To determine how these variables affected the results, five series of samples were made. To create the soil samples, these series blended the contents of fine-grained (clay) and coarse-grained (sand). The percentages of sand that corresponded to the clay contents were 100%, 75%, 50%, 25%, and 0%, respectively. Each series' dielectric characteristics were measured and assessed at five different volumetric water content levels, ranging from 0% to 20%. Three stages of compaction were applied to each sample in order to produce soil samples with three distinct densities at each moisture content and texture level because the physical characteristics of soil, such as density, porosity, and moisture content, are interdependent and influence one another.

Following the preparation of these soil samples, the suggested MADS was used to measure the dielectric characteristics of 75 moist soils. Empirical and AI-based dielectric models were created and assessed for these samples. Since theoretical dielectric models are unable to determine soil density, they were not utilized. The volume fraction of soil phases and the dielectric characteristics of each phase are the only factors considered in theoretical models, such as volumetric mixture models. Ignoring the interactions between phases, they calculate the dielectric properties of soil based on the dielectric properties and volume fractions of each phase. The applicability of theoretical models is limited by the dynamic nature of soil, which is subject to loads that alter its density and the volume of each phase through compaction or consolidation. Consequently, the ensuing subsections will not address or elaborate on this kind of dielectric model.

5.2.1. General empirical dielectric models

The majority of researchers focus on the dielectric characteristics of soil in relation to water content or soil composition. This study produced a number of models that provide good relationships with three different variables: soil texture, density, and moisture content. Table 4 provides a summary of these general models for the clean soil's dielectric constant. Intensive regression analysis performed and many formulas for model the dielectric constant. For each model ANOVA analysis were performed to evaluate and determine the best model to fit the data. The best five model obtained in this study are listed below.

Model 1 (DM1) dielectric constant is function of soil texture (sand content) and soil moisture content (21).

$$\varepsilon'_{soil} = 7.906 - 0.09405S + 1.215\theta - 0.0116\theta^2 + 0.00058\theta^3 \quad (21)$$

Model 2 (DM2) dielectric constant is function of soil density and moisture content (22).

$$\varepsilon'_{soil} = 3.59 - 0.29\rho + 1.220\theta - 0.0114\theta^2 + 0.00057\theta^3 \quad (22)$$

Model 3 (DM3) dielectric constant is function of soil texture (sand content), density and soil moisture content (23).

$$\varepsilon'_{soil} = 0.33 - 0.09967S + 5.87\rho + 1.116\theta - 0.0153\theta^2 + 0.00089\theta^3 \quad (23)$$

Model 4 (DM4) dielectric constant is function of soil texture (sand and clay contents), density and soil moisture content (24).

$$\varepsilon'_{soil} = -0.0963S + 0.0033C + 5.87\rho + 1.116\theta - 0.0153\theta^2 + 0.00089\theta^3 \quad (24)$$

Table 4. ANOVA and regression analysis of empirical dielectric constant models.

Model	R square	R adjusted	Error (RMSE)	F value	Sig.
DM1	0.9090	0.9038	3.0053	174.8	0.000
DM2	0.7896	0.7776	4.5690	65.69	0.000
DM3	0.9158	0.9097	2.9120	150.0	0.000
DM4	0.9756	0.9735	2.9120	7.310	0.009

Table 5 provides a summary of the general models for the clean soil's loss factor. Intensive regression analysis performed and many formulas for model the loss factor. For each model ANOVA analysis were performed to evaluate and determine the best model to fit the data. The best five model obtained in this study are listed below. An example of the dielectric constant and loss factor of soil calculated using model 1 (DM1 and LM1) could be seen in Figure 13.

Model 1 (LM1) loss factor is function of soil texture (sand content) and soil moisture content (25).

$$\varepsilon'_{soil} = 20.92 - 0.3839S + 3.82\theta + 0.262\theta^2 + 0.0123\theta^3 \quad (25)$$

Model 2 (LM2) loss factor is function of soil density and moisture content (26).

$$\varepsilon'_{soil} = -51.1 + 39.5\rho + 3.15\theta + 0.236\theta^2 + 0.0144\theta^3 \quad (26)$$

Model 3 (LM3) loss factor is function of soil texture (sand content), density and soil moisture content (27).

$$\varepsilon'_{soil} = -65.8 - 0.4482S + 67.2\rho + 2.68\theta + 0.218\theta^2 + 0.0159\theta^3 \quad (27)$$

Model 4 (LM4) loss factor is function of soil texture (sand and clay contents), density and soil moisture content (28).

$$\varepsilon'_{soil} = -1.106S - 0.658C + 67.2\rho + 2.268\theta + 0.2180\theta^2 + 0.01591\theta^3 \quad (28)$$

Table 5. ANOVA and regression analysis of empirical loss factor models.

Model	R square	R adjusted	Error (RMSE)	F value	Sig.
LM1	0.9342	0.9305	28.007	248.6	0.000
LM2	0.9204	0.9159	30.811	202.4	0.000
LM3	0.9416	0.9374	26.576	222.6	0.000
LM4	0.9720	0.9696	26.576	399.5	0.000

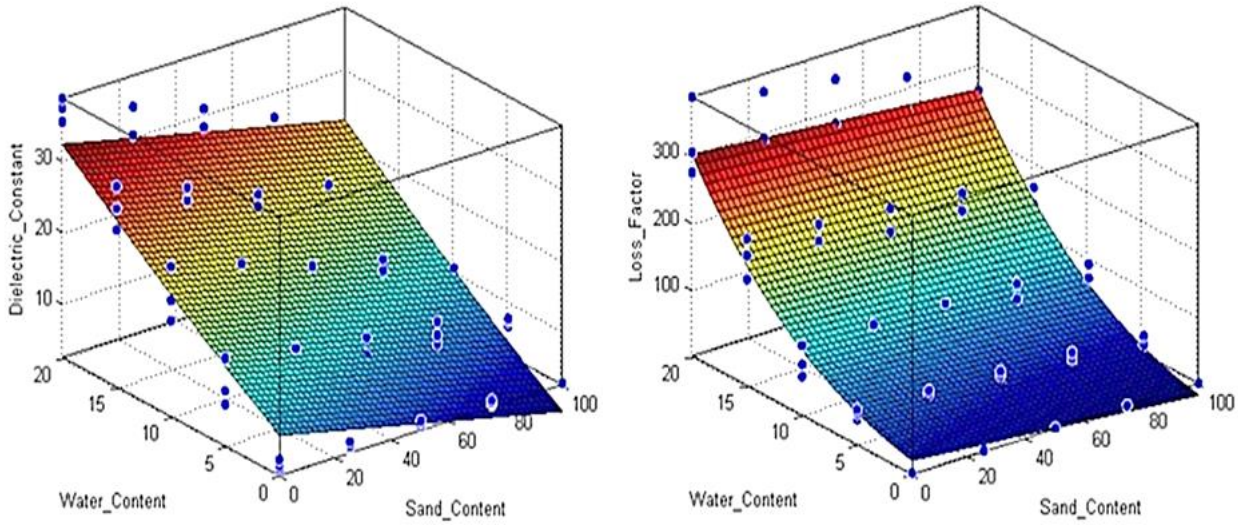

Figure 13. Models of dielectric properties (DM1 and LM1) versus sand and moisture content.

5.2.2. AI dielectric models

Two ANN models were used to predict dielectric properties of moist sand based on the measured loss factor using the proposed sensor. These models are FNN and CNN. The two models used an input layer with four variables (volume fraction of the four soil phases) and one output layer with two variables (sand dielectric constant and loss factor). The FNN model has one hidden layer with six neurons while the CNN model has one hidden layer with twelve neurons. Both models have used the 'logsig' activation function in the input and hidden layers. Both models also used the 'puelin' activation function in the output layers. The training method in both models was the 'levenberg Marquardt' method. The best ANN model was CNN model. The schematic diagram and detail of CNN model is presented in Figure 14. The performance details of the best CNN model is shown in Figure15.

The prediction results of the soil dielectric properties of sandy soil using the ANN model indicated

that both models are excellent in estimating sand dielectric constant. The correlation coefficients (R) of the training phase for FNN and CNN models were 0.9823 and 0.9999 respectively. Therefore, the best ANN was CNN. The R for the validation and testing phase of CNN were 0.9855 and 0.9929, respectively. However, these high correlation coefficients did not account for variables excluded from the study or nonlinearity. ANN, on the other hand, effectively captured nonlinear effects and considered additional factors that were not included in the original study. To evaluate the reliability of the ANN models, several rounds of random training were performed. This approach ensured that the favorable results were not merely coincidental or dependent on a particular training instance. Importantly, the correlation coefficients (R) remained consistent across the different training trials, indicating stable and reliable model performance.

6. Limitation and future work

Although the results of this study demonstrate that both ANN models, including cascade feedforward neural networks (CNN) and feedforward neural networks (FNN), exhibit high predictability for the soil moisture content and soil dielectric properties, future work should include a sensitivity analysis of these neural methods. Additionally, other AI techniques such as machine learning, XGBoost, the black widow optimization method, and convolutional neural networks could be explored [67]. Moreover, nonlinear regression analysis and response surface methodology could be applied, incorporating more soil data and soil condition such as soil pollution, salt content, salinity, to improve the results and compare these methods with various ANN approaches. Future work could consider some recent advances on the parsimony, interpretability and predictive capability of a physically-based model in the optical domain for estimating soil moisture content [68].

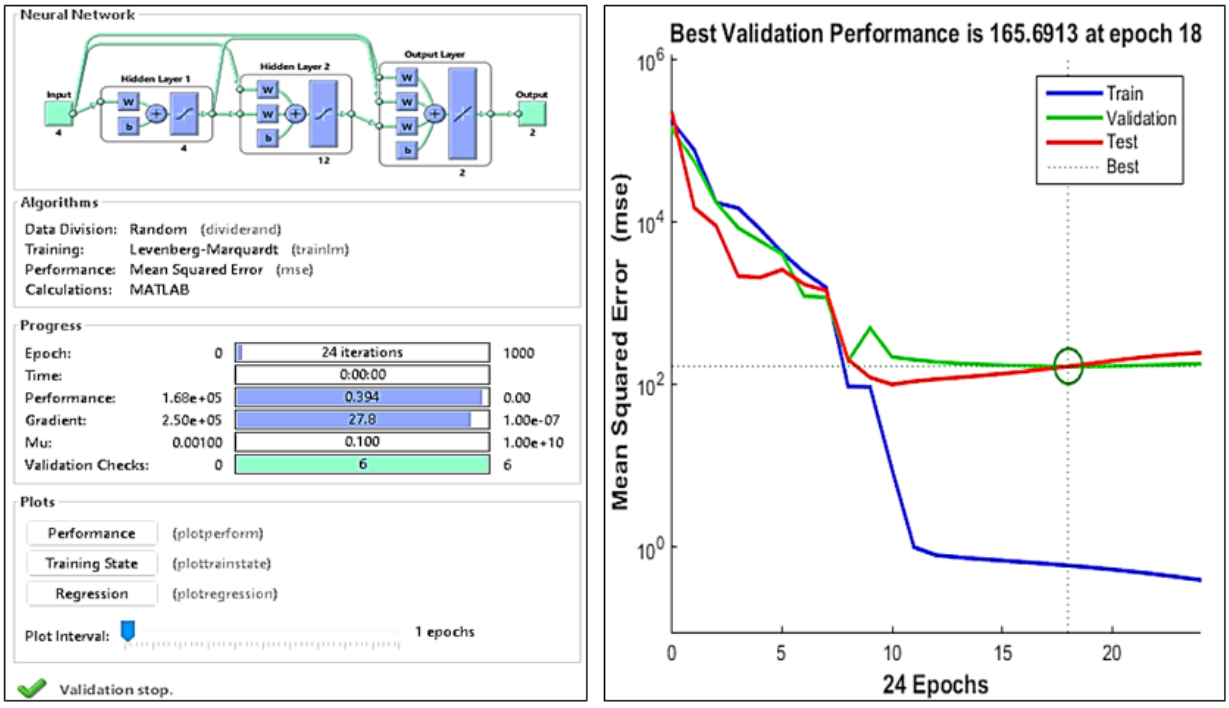

Figure 14. The detail of CNN model used to predict soil dielectric properties.

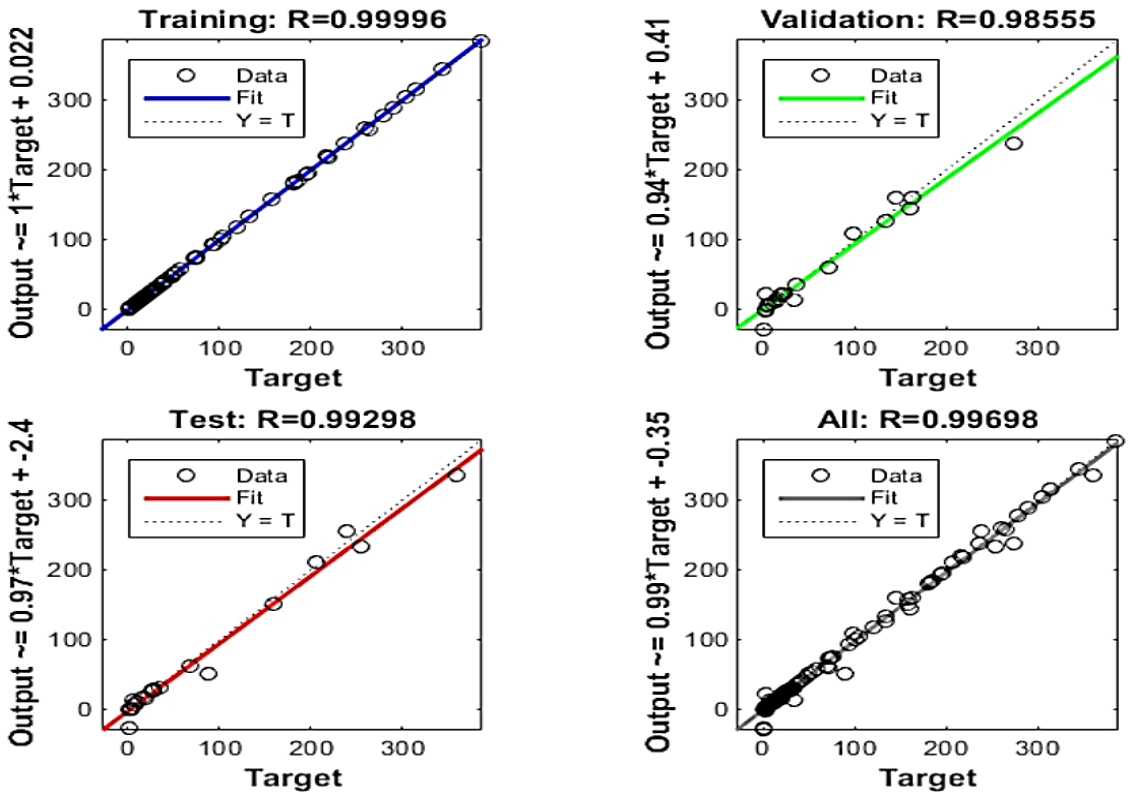

Figure 15. Experimental soil dielectric properties versus predicted values using CNN model.

7. Conclusions

To characterize dielectric properties in situ as well as in the lab, the multi array electromagnetic sensor (MAES) was developed. The MAES is a low-cost, lightweight, easy to use, portable, and user-friendly instrument for precisely measuring dielectric properties in the field and in the lab. The sensor's multiple electrodes allow it to measure the moisture profile and the dielectric profile of the soil in relation to its depth. Furthermore, the sensor was calibrated and validated for accurate dielectric measurement of soil. This study also evaluates three types of dielectric models used for estimation soil moisture content. These models include theoretical volumetric mixture models and statistical empirical models. The results obtained in this study can be lead to the following concluded points:

- Theoretical models such as volumetric mixture models can be used only for coarse grain soil (sandy soil). The measured of dielectric properties of moist sandy soil was under estimate of dielectric properties specially at higher moister content. The best model was Silberstein's linear model. A new theoretical model based on power formula was developed. This model indicates the best fitting theoretical model for dielectric constant of moist sand with power equal to 0.9 and for loss factor the best power was 1.4. All theoretical models cannot be used and not applicable for general soil in practice were soil could possess different texture and different densities.
- New statistical regression models were developed for sandy soil. These models include linear, quadratic and cubic formula. The best model was the cubic formula having correlation coefficients 0.993 for dielectric constant and 0.997 for loss factor.
- For general soil with different soil texture (clay and sand), different density and different moisture

content, four new statistical empirical models were developed to take into account the density, texture, and moisture the best model was the fourth model with high correlation coefficient 0.975 for dielectric and 0.972 for loss factor. These new models can solve the problem from recalibration of soil measurement based on dielectric measurement for soil.

- Furthermore, this study investigates to develop and AI using ANN models for dielectric properties of soil. The ANN models indicate the high capability of modeling dielectric properties of mist soil for both sand soil and general soil. The best ANN model for sand dielectric properties was FNN model with correlation coefficients of 0.9999 for training data and 0.997 for testing and validation. The best ANN for general soil dielectric properties was the CNN model with correlation coefficients 0.9999 for training data and 0.996 for testing. However, these high correlation coefficients did not account for variables excluded from the study or nonlinearity. ANN, on the other hand, effectively captured nonlinear effects and considered additional factors that were not included in the original study.

Use of AI tools declaration

The authors declare they have not used Artificial Intelligence (AI) tools in the creation of this article.

Acknowledgments

The researchers' express gratitude for the support provided by the Research Deanship and the Faculty of Engineering at Yarmouk University.

Conflict of interest

The authors declare no conflict of interest.

Authors Contribution

All authors contributed equally to the manuscript. All authors wrote the manuscript, conducted the experimental testing, performed empirical models, reviewed the manuscript, and helped in the result analysis. Yaser Jaradat primarily contributed to the editing and review of the revised version of this study. Additionally, he conducted the sensitivity analysis, performing multiple rounds of random training for the ANN.

References

1. Derakhti A, Santibanez Gonzalez EDR, Mardani A (2023) Industry 4.0 and Beyond: A Review of the Literature on the Challenges and Barriers Facing the Agri-Food Supply Chain. *Sustainability* 15: 5078. https://doi.org/10.3390/su15065078
2. Jiang M, He L, Niazi NK, et al. (2023). Nanobiochar for the remediation of contaminated soil and water: Challenges and opportunities. *Biochar* 5: 2. https://doi.org/10.1007/s42773-022-00201-x
3. Zhang X, He L, Yang X, et al. (2023) Editorial: Soil pollution, risk assessment and remediation. Front. *Environ Sci* 11:1252139. https://doi.org/10.3389/fenvs.2023.1252139

4. Rasheed MW, Tang J, Sarwar A, et al. (2022) Soil Moisture Measuring Techniques and Factors Affecting the Moisture Dynamics: A Comprehensive Review. *Sustainability* 14: 11538. https://doi.org/10.3390/su141811538
5. Schreiber ME, Cozzarelli IM (2021) Arsenic release to the environment from hydrocarbon production, storage, transportation, use and waste management. *J Hazard Mater* 411: 125013. https://doi.org/10.1016/j.jhazmat.2020.125013
6. ASTM Standard D2216-19 (2019) Standard test methods for laboratory determination of water (moisture) content of soil and rock by mass. ASTM International, West Conshohocken, PA.
7. Zhang L, Meng Q, Hu D, et al. (2020). Comparison of different soil dielectric models for microwave soil moisture retrievals. *Int J Remote Sens* 41: 3054–3069. https://doi.org/10.1080/01431161.2019.1698077
8. Howells OD, Petropoulos GP, Triantakonstantis D, et al. (2023) Examining the variation of soil moisture from cosmic-ray neutron probes footprint: experimental results from a COSMOS-UK site. *Environ Earth Sci* 82: 41. https://doi.org/10.1007/s12665-022-10721-1
9. Marica Baldoncini, Matteo Albéri, Carlo Bottardi, et al. (2019) Fabio Mantovani, Biomass water content effect on soil moisture assessment via proximal gamma-ray spectroscopy. *Geoderma* 335: 69–77.
10. Pires LF, Cássaro FAM (2023) Nuclear Laboratory Setup for Measuring the Soil Water Content in Engineering Physics Teaching Laboratories. *Agri Engineering* 5: 1079–1089.
11. Oiganji Ezekiel, B. A. Danbaki, G. T. Fabumi. (2021) Performance evaluation of gypsum block, tensiometer sensor for soil moisture content determination. *J Agri Engin Technol* 26: 102–111.
12. Abdulraheem MI, Chen H, Li L, et al. (2024) Recent Advances in Dielectric Properties-Based Soil Water Content Measurements. *Remote Sens* 16:1328. https://doi.org/10.3390/rs16081328
13. Celik MF, Isik MS, Yuzugullu O, et al. (2022) Soil Moisture Prediction from Remote Sensing Images Coupled with Climate, Soil Texture and Topography via Deep Learning. *Remote Sens* 14: 5584.
14. Bittelli K, Flury M (2009) Errors in water retention curves determined with pressure plates. *Soil Sci Soc Am J* 72: 1453–1460.
15. Cheng O, Su Q, Binley A, et al. (2023) Estimation of Surface Soil Moisture by a Multi-Elevation UAV-Based Ground Penetrating Radar. *Water Resour Res* 59: 2.
16. Egor AO, Agwul AA, Asu BS (2023) The use of ground penetrating radar (GPR) method in the evaluation of soil moisture content of parts of cross river central soil for precision agriculture in South-south Nigeria. *Int J Sci Res Arch* 9: 392–403. https://doi.org/10.30574/ijsra.2023.9.2.0564
17. Cui F, Ni J, Du Y, et al. (2021). Soil water content estimation using ground penetrating radar data via group intelligence optimization algorithms: An application in the Northern Shaanxi Coal Mining Area. *Energ Explor Exploit* 39: 318–335.
18. Ismail R, Al-Mattarneh H, Malkawi AB, et al. (2024) Prediction Moisture Content and Strength of Wood Using Free-Space Microwave Transmission Line NDT. 2024 21st International Multi-Conference on Systems, Signals and Devices, SSD 2024, 492–499. https://doi.org/10.1109/SSD61670.2024.10548770
19. Telfah D, Al-Mattarneh H, Ismail R, et al. (2024) Development of permittivity sensor for advanced in situ testing and evaluation of building material. 2024 21st International Multi-Conference on Systems, Signals and Devices, SSD 2024, 164–169. https://doi.org/10.1109/SSD61670.2024.10548329

20. Al-Mattarneh HMA, Ghodgaonkar DK, Majid WMBWA (2001) Determination of compressive strength of concrete using free-space reflection measurements in the frequency range of 8–12.5 GHz. Asia-Pacific Microwave Conference Proceedings, APMC 2: 679 - 682.
21. Al-Mattarneh HMA, Ghodgaoankar DK, Abdul Hamid H, et al. (2002) Microwave reflectometer system for continuous monitoring of water quality. 2002 Student Conference on Research and Development: Globalizing Research and Development in Electrical and Electronics Engineering, SCOReD 2002 - Proceedings, art. no. 1033150, 430–433. https://doi.org/10.1109/SCORED.2002.1033150
22. Dahim M, Abuaddous M, Ismail R, et al. (2020) Using a dielectric capacitance cell to determine the dielectric properties of pure sand artificially contaminated with Pb, Cd, Fe, and Zn. *Appl Environ Soil Sci* 2020: art. no. 8838054. https://doi.org/10.1155/2020/8838054
23. Al-Mattarneh HMA, Ghodgaonkar DK, Majid WMBWA (2001) Microwave nondestructive testing for classification of Malaysian timber using free-space techniques. 6th International Symposium on Signal Processing and Its Applications, ISSPA 2001 - Proceedings; 6 Tutorials in Communications, Image Processing and Signal Analysis, 2, art. no. 950177, pp. 450–453. https://doi.org/10.1109/ISSPA.2001.950177
24. Al-Mattarneh H, Alwadie A (2016) Development of Low Frequency Dielectric Cell for Water Quality Application. *Procedia Engineering* 148: 687–693. https://doi.org/10.1016/j.proeng.2016.06.554
25. Al-Mattarneh H, Dahim M (2021) Comparison of nondestructive testing method for strength prediction of asphalt concrete material. *Civil Eng J* 7: 165–178. https://doi.org/10.28991/cej-2021-03091645
26. Ismail R, Dahim D, A Jaradat, et al. (2021) Field Dielectric Sensor for Soil Pollution Application. *IOP Conference Series: Earth Environ Sci* 801: 012003.
27. Nuruddin MF, Malkawi AB, Fauzi A, et al. (2016) Effects of alkaline solution on the microstructure of HCFA geopolymers. Engineering Challenges for Sustainable Future - Proceedings of the 3rd International Conference on Civil, offshore and Environmental Engineering, ICCOEE 2016, 501–506. https://doi.org/10.1201/b21942-102
28. Dahim M, Abuaddous M, Al-Mattarneh H, et al. (2021) Enhancement of road pavement material using conventional and nano-crude oil fly ash. *Appl Nanosci* 11: 2517–2524. https://doi.org/10.1007/s13204-021-02103-z
29. Lal P, Shekhar A, Gharun M, et al. (2023) Spatiotemporal evolution of global long-term patterns of soil moisture. *Sci Total Environ* 867: 161470. https://doi.org/10.1016/j.scitotenv.2023.161470
30. Mane S, Das N, Singh G, et al. (2024) Advancements in dielectric soil moisture sensor Calibration: A comprehensive review of methods and techniques. *Comput Electron Agr* 218: 108686. https://doi.org/10.1016/j.compag.2024.108686
31. Hippel AV (1995). Dielectric Materials and Applications, Artech House.
32. Nimer H, Ismail R, Rawashdeh A, et al. (2024) Artificial Intelligence Using FFNN Models for Computing Soil Complex Permittivity and Diesel Pollution Content. *Civil Engin J* 10: 3053–3069.
33. Blanchy G, McLachlan P, Mary B, et al. (2024) Comparison o multi-coil and multi-frequency frequency domain electromagnetic induction instruments. *Front Soil Sci* 4: 1239497. https://doi.org/10.3389/fsoil.2024.1239497

34. Dobriyal P, Qureshi A, Badola R, et al. (2012) A review of the methods available for estimating soil moisture and its implications for water resource management. *J Hydrol* 458: 110–117. https://doi.org/10.1016/j.jhydrol.2012.06.021
35. Pandey G, Weber RJ, Kumar R (2018) Agricultural Cyber-Physical System: In-Situ Soil Moisture and Salinity Estimation by Dielectric Mixing. *IEEE Access* 6: 43179–43191.
36. Mironov VL, Kosolapova LG, Fomin SV (2009) Physically and Mineralogically Based Spectroscopic Dielectric Model for Moist Soils. *IEEE T Geosci Remote* 47: 2059–2070. https://doi.org/10.1109/TGRS.2008.2011631
37. van Dam RL, Borchers B, Hendrickx JMH (2005) Methods for prediction of soil dielectric properties: a review. *Proc of SPIE* 5794: 188–197. https://doi.org/10.1117/12.602868
38. Umoh GV, Leal-Perez JE, Olive-Méndez SF, et al. (2022) Complex dielectric function, Cole-Cole, and optical properties evaluation in BiMnO3 thin-films by Valence Electron Energy Loss Spectrometry (VEELS) analysis. *Ceram Int* 48: 22141–22146. https://doi.org/10.1016/j.ceramint.2022.04.212
39. Hong T, Tang Z, Zhou Y, et al. (2019) Dielectric relaxation of interacting/polarizable polar molecules with linear reaction dynamics in a weak alternating field. *Chem Phys Lett* 727: 66–71. https://doi.org/10.1016/j.cplett.2019.04.053.
40. Sihvola (1999) Electromagnetic Mixing Formulas and Applications. The Institution of Eng. and Tech. UK, London.
41. Birchak J R, Gardner C G, Hipp J E, et al. (1974) High dielectric constant microwave probes for sensing soil moisture. *Proc IEEE* 62: 93–98.
42. Looyenga (1965) Dielectric constants of mixtures. *Physica* 31: 401–406.
43. Zakri T, Laurent JP, Vauclin M (1998) Theoretical evidence for 'Lichtenecker's mixture formulae' based on the effective medium theory. *J Phys D Appl Phys* 31: 1589–1594.
44. Topp GC (2003) State of the art of measuring soil water content. *Hydrol Proces* 17: 2993–2996.
45. Monjardin CEF, Power C, Senoro DB, et al. (2023) Application of Machine Learning for Prediction and Monitoring of Manganese Concentration in Soil and Surface Water. *Water* 15: 2318. https://doi.org/10.3390/w15132318
46. Pham TB, Singh SK, Ly HB (2020) Using Artificial Neural Network (ANN) for prediction of soil coefficient of consolidation. *Vietnam J Earth Sci* 42: 311–319. https://doi.org/10.15625/0866-7187/42/4/15008
47. Ayoubi S, Pilehvar A, Mokhtari P, et al. (2011) Application of Artificial Neural Network (ANN) to Predict Soil Organic Matter Using Remote Sensing Data in Two Ecosystems. *Biomass Remote Sens Biomass*. InTech, 181–196.
48. Carvalho MG, Barreto EMR, Ferreira JAC, et al. (2022) Applications of artificial intelligence in determining soil shear strength parameters: a systematic literature mapping. *Res Soc Develop* 11: e27711124506. https://doi.org/10.33448/rsd-v11i1.24506
49. Negiş H (2024) Using Models and Artificial Neural Networks to Predict Soil Compaction Based on Textural Properties of Soils under Agriculture. *Agriculture* 14: 47. https://doi.org/10.3390/agriculture14010047
50. Li B, You Z, Ni K, et al. (2024) Prediction of Soil Compaction Parameters Using Machine Learning Models. *Appl Sci* 14: 2716. https://doi.org/10.3390/app14072716

51. Han H, Choi C, Kim J, et al. (2021) Multiple-Depth Soil Moisture Estimates Using Artificial Neural Network and Long Short-Term Memory Models. *Water* 13: 2584. https://doi.org/10.3390/w13182584
52. Wrzesiński G, Markiewicz A (2022) Prediction of Permeability Coefficient k in Sandy Soils Using ANN. *Sustainability* 14: 6736. https://doi.org/10.3390/su14116736
53. Bieganowski A, Józefaciuk G, Bandura L, et al. (2018) Evaluation of Hydrocarbon Soil Pollution Using E-Nose. *Sensors* 18: 2463. https://doi.org/10.3390/s18082463
54. Wang Z, Zhang W, He Y (2023) Soil Heavy-Metal Pollution Prediction Methods Based on Two Improved Neural Network Models. *Appl Sci* 13: 11647. https://doi.org/10.3390/app132111647
55. Luo H, Li Y, Gao X, et al. (2023) Carbon emission prediction model of prefecture-level administrative region: A land-use-based case study of Xi'an city, China. *Appl Energ* 348: 121488. https://doi.org/10.1016/j.apenergy.2023.121488.
56. Luo H, Gao X, Liu Z, et al. (2024) Real-time Characterization Model of Carbon Emissions Based on Land-use Status: A Case Study of Xi'an City, China. *J Clean Prod* 434: 140069. https://doi.org/10.1016/j.jclepro.2023.140069.
57. Ismail R, Alsadi J, Hatamleh R, et al. Employing CNN and black widow optimization for sustainable wastewater management in an environmental engineering context. *Asian J Civ Eng* 25: 3973–3988. https://doi.org/10.1007/s42107-024-01024-w
58. Yaseen ZM, Sulaiman SO, Deo RC, et al. (2019) An enhanced extreme learning machine model for river flow forecasting: State-of-the-art, practical applications in water resource engineering area and future research direction. *J Hy* 569: 387–408. https://doi.org/10.1016/j.jhydrol.2018.11.069
59. Ismail R (2024) Improving wastewater treatment plant performance: an ANN-based predictive model for managing average daily overflow and resource allocation optimization using Tabu search. *Asian J Civ Eng* 25: 1427–1441. https://doi.org/10.1007/s42107-023-00853-5
60. Ismail R, Rawashdeh A, Al-Mattarneh H, et al. (2024) Artificial Intelligence for Application in Water Engineering: The Use of ANN to Determine Water Quality Index in Rivers. *Civ Eng J* 10: 2261–2274. http://dx.doi.org/10.28991/CEJ-2024-010-07-012
61. Al-Mattarneh H, Ismail R, Albtoush F (2024) Monitoring concrete curing and strength using microwave waveguide sensor and ANN, AEIT2024 International Annual Conference, Trento, Italy, 25–27 September, 2024.
62. Al-Mattarneh H, Rawashdeh A, Ismail R (2024) Quantifying the moisture content of transformer oil using dielectric properties and artificial intelligence, AEIT2024 International Annual Conference, Trento, Italy, 25–27 September, 2024.
63. Agilent Technologies Inc. (2008) Agilent 4285A, Precision LCR Meter, Data Sheet, Printed in USA, November 12, 5963–5395E.
64. Nimer H, Ismail R, Al-Mattarneh H, et al. (2025) Artificial neural networks and noncontact microwave NDT for evaluation of polypropylene fiber concrete. *Asian J Civ Eng* 26: 273–292. https://doi.org/10.1007/s42107-024-01189-4
65. Zain MFM, Karim MR, Islam MN, et al. (2015) Prediction of strength and slump of silica fume incorporated high-performance concrete. *Asian J Sci Res* 8: 264–277. https://doi.org/10.3923/ajsr.2015.264.277

66. Al-Mattarneh H, Abuaddous M, Ismail R, et al. (2024) Performance of concrete paving materials incorporating biomass olive oil waste ash and nano-silica. *AIMS Mater Sci* 11: 1035–1055. https://doi.org/10.3934/matersci.2024049
67. Güllü H, Fedakar, HI (2017) On the prediction of unconfined compressive strength of silty soil stabilized with bottom ash, jute and steel fibers via artificial intelligence. *Geomechanics and Eng* 12: 441–464.
68. Penland C, Fowler MD, Jackson DL, et al. (2021) Forecasts of Opportunity for Northern California Soil Moisture. *Land* 10: 713. https://doi.org/10.3390/land10070713

AIMS Press